

A. WÓJCIK^{1*}, R. CHULIST¹, A. SZEWCZYK¹, J. DUTKIEWICZ¹, W. MAZIARZ¹**THE INFLUENCE OF γ' PRECIPITATES ON THE STRUCTURAL STABILITY OF FENICOALTA AND FENICOALTAB SINGLE CRYSTALS AFTER CYCLIC SUPERELASTIC DEFORMATION**

Two single crystals with compositions Fe-Ni-Co-Al-Ta and Fe-Ni-Co-Al-Ta-B were selected and fabricated by Bridgman method. Subsequently, ingots were homogenized, oriented and subjected to a two-step heat treatment process in order to obtain fine and coherent γ' precipitates. Subsequently, superelastic cycling experiments were performed at 77 K. The next step included detailed microstructural characterization using transmission electron microscopy and high-energy synchrotron X-ray diffraction measurements together with Rietveld refinement. The results show that the number of fully reversible superelastic strains is very sensitive to the size of γ' precipitates. The smaller (3 nm) γ' precipitates ensured more superelastic response compared to material with larger γ' particles size (5 nm), in which the material did not receive its original shape after 10 cycles even after being heated.

Keywords: Fe-based shape memory alloys; superelastic effect; cyclic deformation; TEM

1. Introduction

Among the intensively studied groups of functional materials, such as Nitinol or Ni-Mn-Ga, Ni-Mn-Sn and Ni-Fe-Ga Heusler alloys, Fe-based alloys are attractive due to: (i) low production cost, (ii) high strength, (iii) good cold formability and workability, and (iv) high magnetization change between the austenitic and martensitic phases. Moreover, Fe-based materials show excellent ability to accommodate plastic deformations without brittle fracture, ensuring high repeatability of superelastic and elastocaloric cycles [1-7]. Martensitic transformation in Fe-based alloys takes place between the high-temperature austenitic phase γ (*fcc*) and the low-temperature martensitic phase $L1_0$ (*bct*) whereas is strictly controlled by the γ' ($L1_2$) phase precipitates introduced by additional heat treatment changing the character of martensitic transformation from non-thermoelastic to thermoelastic type [8,9]. Moreover, the size, volume fraction and degree of coherency of the γ' precipitates have a significant influence on the occurrence and the temperature range of martensitic transformation and consequently the magnitude of superelastic effect. Tanaka et al. showed that the polycrystalline alloy with a strong $\{035\} \langle 100 \rangle$ recrystallization texture, after rolling process exhibits a large superelastic strain of about 13.5%. This value is twice as high as that obtained for materials based on Ni-Ti [10]. In turn, Kainuma et al. investigated a Fe-Ni-Co-Al-

Nb-B polycrystalline alloy in which a superelastic effect of over 5% was observed [11]. Many studies concerned the influence of heat treatment on the morphology, size and volume fraction of the γ' phase, as well as the formation of additional phases, which directly affects the size of the superelastic effect [12-20]. It has been reported that Fe-Ni-Co-Al-Ta single crystal, heat treated at 973 K for 0.5 h shows the maximum value of the superelastic effect of about 15.7% [18-20]. Such a level of superelastic strain can be obtained in material with the γ' precipitate size of approx. 5 nm and volume fraction close to 4 vol.%. It was also found that extending heat treatment time increases the size and volume fraction of the γ' precipitates, which in time leads to the formation of an additional, brittle β phase. This phase is uncoherent and negatively influences the magnitude and reversibility of the superelastic effect [18]. In turn, a small addition of boron (0.05 at.%) in NCATB single crystals strongly inhibits the formation of the β phase, even in single crystals annealed over longer times (24 h). Moreover, the B doping reduces the average size of the γ' precipitates to about 3-4 nm having a positive effect on the magnitude and reversibility of the superelastic effect [18,19]. A thorough analysis of the γ' precipitates was performed by Ma et al. using atom probe tomography and transmission electron microscopy in order to determine its size, volume fraction, and distribution. It was found that the formation of an additional γ' and β phases influences the chemical composition of the matrix,

¹ INSTITUTE OF METALLURGY AND MATERIALS SCIENCE, 25 REYMONTA STR., 30-059 KRAKOW, POLAND

* Corresponding author: a.wojcik@imim.pl



changing the concentration of valence electrons (e/a), and thus leading to a change in the temperature range of martensitic transformation [13,14]. Similar conclusions were made by Czerny et al. [18], which indicate a strong shift of the martensitic transformation temperature towards higher temperatures along with the formation of a large amount of β phase. This was caused by the change in the value of e/a (depletion of Ni and Al and enrichment in Fe and Co in the matrix) [18,20].

In this work, two single crystalline alloys: Fe-28Ni-17Co-11.5Al-2.5Ta (NCAT) and Fe-28Ni-17Co-11.5Al-2.5Ta-0.05B (NCATB) with various volume fraction and size of γ' precipitations were selected. Samples were chosen in such a way that they exhibit different superelastic responses. Based on the graph shown in [21], three characteristic areas (super-elastic, mechanical stabilization, and elasto-plastic) can be marked depending on the size of the γ' precipitates. Precipitates within the range of 3-5 nm are beneficial for fully reversible superelastic behaviour while the larger ones stabilize martensite structure giving rise to the so-called mechanical stabilization [21]. This effect is directly related to the single variant state in martensite which on the microstructure level requires formation of a compatible austenite/twinned martensite interface increasing the nucleation barrier for austenite. In simple terms, it shifts the austenite start temperature to higher values. Nevertheless, such samples exhibit superelastic effect, however, in addition to stress release they require heating. Hence, two alloys from the superelastic range were selected for further research. The main aim of the work was to investigate the impact of the lack of austenite/twinned martensite interfaces on cyclic stability of Fe-based single crystalline shape memory alloys.

2. Experimental

The single crystals with compositions of Fe-28Ni-17Co-11.5Al-2.5Ta (NCAT) and (ii) Fe-28Ni-17Co-11.5Al-2.5Ta-0.05B (all in at.%) (NCATB) were grown by Bridgman method. The preparation of alloys was described in our previous works [18-21]. The single crystalline samples of [100](001) orientation of the *fcc* austenite phase were cut into $3 \times 3 \times 10 \text{ mm}^3$. Subsequently, single crystals were subjected to two-step heat treatment: (1) annealing at 1573 K/1h followed by water quenching and (2) aging treatment at 973 K/0.5 h followed by cooling in ice water.

High-energy X-ray diffraction measurements were used in order to determine the phase composition and volume fraction of the individual phases. The X-ray diffraction measurements were performed at Petra III DESY Hamburg synchrotron using beamline P07B (87.1 keV, $\lambda = 0.0142342 \text{ nm}$) and 2D Mar345 Image Plate detector in the so-called continuous mode allowing for investigation in transmission geometry which ensure good statistic (beam size $0.8 \times 0.8 \text{ mm}^2$) [22,23]. Moreover, the samples were continuously rotated 180° around the ω -axis (about 6° away from $\langle 100 \rangle$) during the measurements to get rid of the texture (orientation) effect. Subsequently, 2D diffraction patterns were converted into 2Theta/Intensity profiles with

Fit2D software. The microstructure and chemical composition were investigated by Tecnai G2 operating at 200 kV equipped with an energy dispersive X-ray (EDX) microanalyzer and a high angle annular dark field detector (HAADF). Thin foil samples for TEM observations were prepared with TenuPol-5 double jet electropolisher using an electrolyte of perchloric acid (20%) and ethanol (80%) at 253 K with a voltage of 20 V. Additionally, just before the observations, the samples were thinned with the Leica EM RES 101 ion milling machine. Superelastic cycling experiments (up to 10 cycles) were performed at temperature of liquid nitrogen. The preliminary compression tests for both single crystals were performed and published in our previous works [18-21].

3. Results and discussion

3.1. Superelastic properties

Fig. 1 shows the cyclic stress-strain response of the NCAT alloy recorded at liquid nitrogen temperature (the insert shows the stress-strain curve after the first superelastic cycle [21]). The NCAT initial alloy shows a fully reversible superelastic strain of about 15% [21]. This value exceeds subtly the theoretical strain indicating that the entire sample volume, including matrix and γ' precipitates, transformed into martensite indicating that lattice parameters of NCAT single crystal may slightly vary from that measured at room temperatures. The stress-strain curve shows two “humps” with maximum values at 500 MPa and 400 MPa. The first one corresponds to the onset of martensitic transformation while the second one may be related to the reorientation of the martensite variants. Interestingly, the deformation is permanent at the temperature of liquid nitrogen, and the sample returns to its original state when heated to 123 K. This effect is called mechanical stabilization and as it was mentioned is connected with the single variant state of martensite. Additionally, the stress for the onset of martensitic transformation after each cycle was determined and presented in table (Fig. 1b). It can be clearly visible that the stress onset of the martensitic transformation decreases steadily with each cycle being a consequence of the mechanical training. It should be noted that the reverse martensitic transformation in NCAT single crystals is fully reversible and occurs rapidly when heating the sample.

The NCATB single crystal was also subjected to cyclic stress-strain tests. Fig. 2 shows a set of stress-strain curves for NCATB single crystals up to 10 superelastic cycles, the inset presents the superelastic response of the initial alloy [22]. The value of a superelastic strain is found to be 14.3%. The addition of a small amount of boron increases the onset stress of the martensitic transformation from about 500 to 600 MPa for the sample after the first superelastic cycle. Moreover, the addition of B allows for a fully reversible superelastic response at the temperature of 77 K. Similarly to NCAT, with each cycle, the onset stress of the martensitic transformation decreases reaching 218 MPa after 10 superelastic cycles (table: Fig. 2b). The

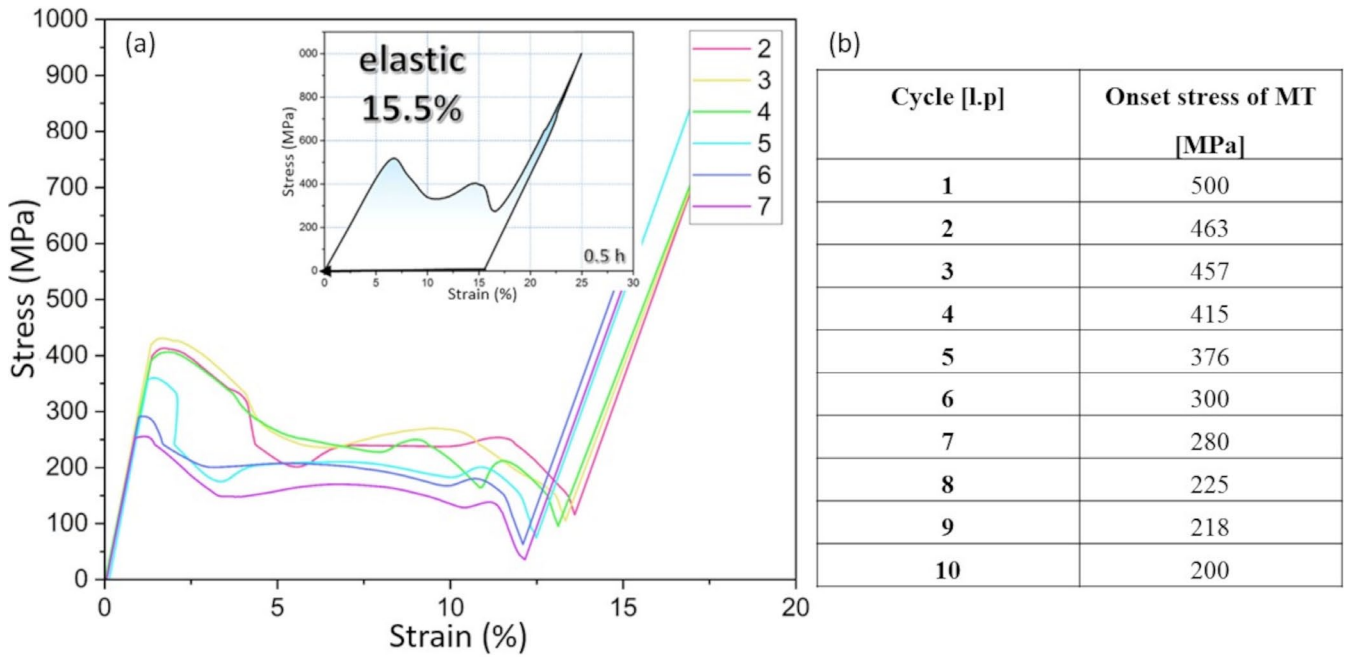


Fig. 1. (a) Cyclic superelastic response of NCAT alloys, (b) dependence of onset stress of MT on the number of superelastic cycles

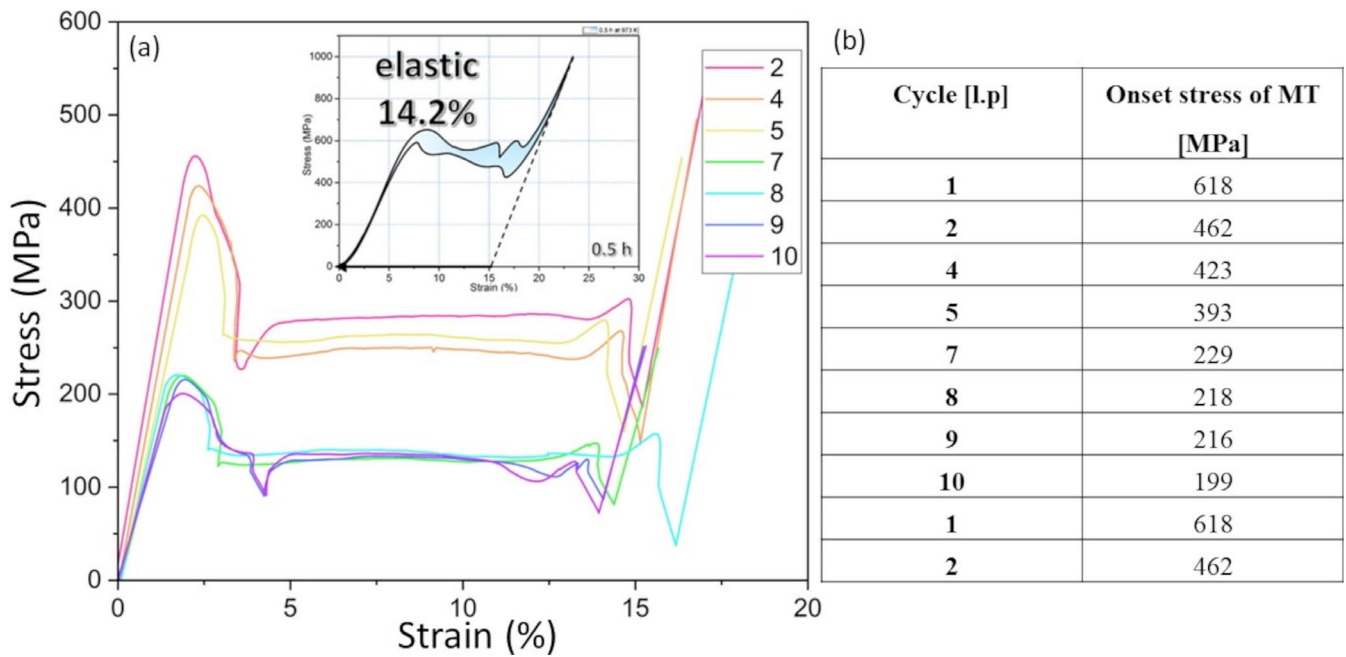


Fig. 2. (a) Cyclic superelastic response of NCATB alloys, (b) dependence of onset stress of MT on the number of superelastic cycles

stress-strain curve after the release of an applied load was not registered because after loading the sample was taken out to measure the As temperature.

3.2. Microstructure

The NCAT base alloy shows a two-phase microstructure consisting of γ austenite (fcc) and γ' precipitates ($L1_2$, Ni_3Al -type). Based on Rietveld and TEM analysis, the volume fraction of γ' phase is estimated to be 4 vol.% while the mean size

of precipitates reaches of about 5 nm (2-6 nm). In the case of NCATB single crystal, the size of γ' precipitates is determined to be 3 nm with the volume fraction at the level of 2 vol.%. Here, the vol.% of γ' phase is two times lower compared to the NCAT single crystal which is related to the B addition located in the interstitial positions and consequently inhibiting diffusion during the aging process.

Fig. 3 presents RT high energy X-ray diffraction patterns of NCAT alloy after 7 (green curve) and 10 (black curve) superelastic cycles as well as NCATB after 10 (red curve) superelastic cycles. The NCAT sample after 7 compression cycles (the sample

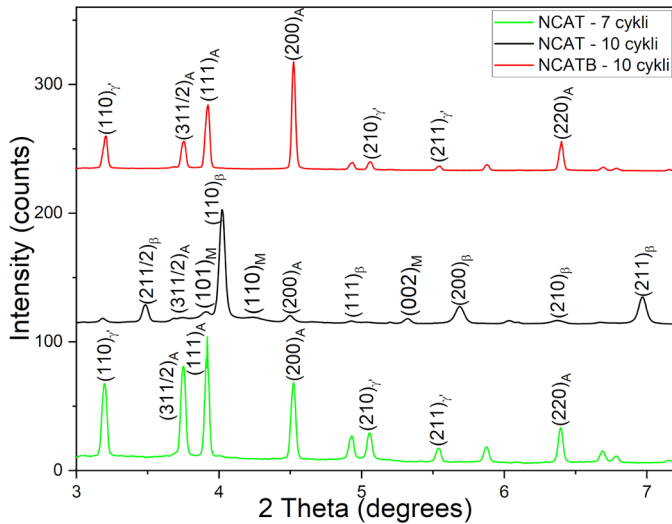


Fig. 3. High energy X-Ray diffraction patterns of NCAT and NCATB alloys after 7 and 10 superelastic cycles collected at RT

returned to its initial state at room temperature) is characterized by a two-phase microstructure consisting of the γ austenite and an additional γ' phase. Moreover, the Rietveld analysis shows a greater amount of γ' phase at the level of about 6.7 vol.% with respect to the initial alloy. However, in the case of the sample subjected to 10 compression cycles the sample does not recover its original shape, even when heated up to the temperature of 773 K. It seems that each cycle, connected with very abrupt

back transformation, produces a number of defects (mostly dislocations) which impedes austenite nucleation. For instance, this sample subjected to 8th cycle transforms back recovering fully the initial shape at about 323 K and after 9th cycle at about 473 K. However, heating up even to 773 K after 10th cycle does not initiate martensite back transformation. A very short heating (10 min) at 773 K leads instead to the formation of β phase. Diffraction pattern given in Fig. 3 shows high-intensity peaks identified in accordance with the β phase structure (*bcc*, NiAl-type) while low intensity peaks are assigned to the austenitic γ , γ' and martensitic (*bct*) phases. The volume fraction of individual phases, estimated by the Rietveld method, amounts to: β – 80.5%, γ – 9.9%, γ' – 2.1% and martensite – 7.5%. In the case of Fe-based alloys, the existence of the β phase is unfavourable due to large constant misfit giving rise to coherency losses. This in turn reduces the mechanical and superelastic properties. Moreover, the β phase, due to its brittleness, causes degradation of the material. On the other hand, the NCATB sample after 10 superelastic cycles (red curve) is characterized only by γ austenite and γ' phase with a precipitate volume fraction of 4.1 vol.%.

Fig. 4a shows a set of bright field (BF) TEM images and corresponding selected area electron diffraction (SAED) patterns for the NCAT sample after 7 superelastic cycles. SAED confirms the two-phase structure in which yellow reflections correspond to γ austenite while the green ones to the γ' phase. Moreover, the TEM micrographs show a large number of dislocations and a plate of residual martensite (pink arrow) and slip bands. Based

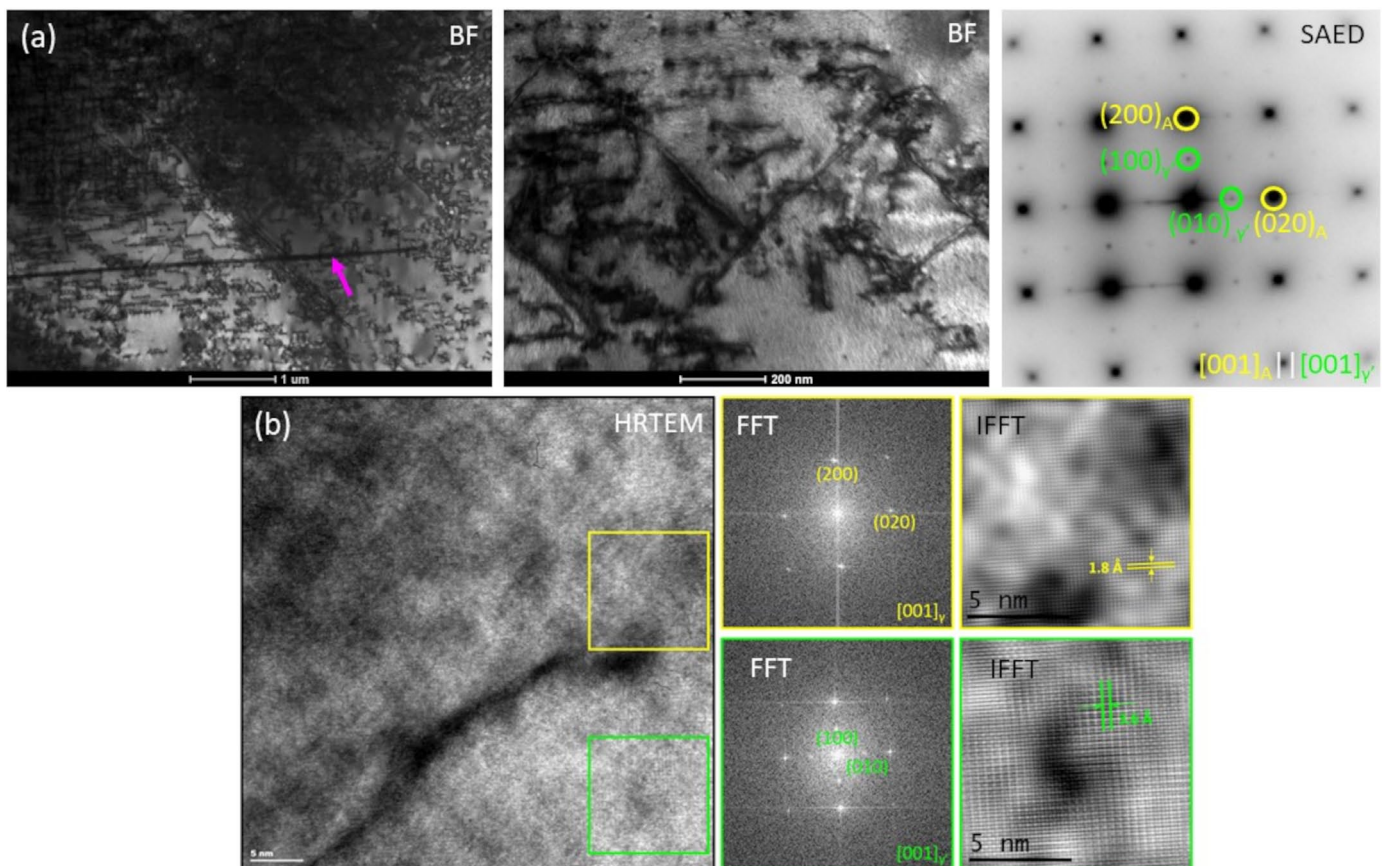


Fig. 4. (a) BF TEM images and corresponding SAED patterns and (b) HRTEM FFT and IFFT images of NCAT sample after 7 superelastic cycles

on the dark field (DF) TEM observations, taken from the $(100)\gamma'$ reflection and high-resolution (HRTEM) images, the average crystallite size is estimated to be 5 nm, which is consistent with the results obtained for the initial sample. Fig. 4b shows the HRTEM together with Fast Fourier Transform (FFT) and Inverse Fast Fourier Transform (IFFT) images, for the NCAT sample after 7 compression cycles, taken from two areas. The yellow square is generated from the area without precipitates while the FFT image shows reflections corresponding only to γ austenite. However, fine γ' precipitates are clearly visible in the region marked by green, which is confirmed in the FFT image where the additional $\{100\}$ peaks belong to the ordered γ' phase. The IFFT taken from the green area shows an extra $\{100\}$ plane with 3.61 Å lattice parameter while the IFFT image generated from the yellow presents only $\{200\}$ planes with 1.8 Å spacing. Moreover, HRTEM images confirm a good coherency between the precipitates and the matrix. As demonstrated by synchrotron X-ray diffraction measurements, the microstructure of NCAT alloy after 10 superelastic cycles consists of the β phase, with a small amount of residual austenite and martensite.

A series of BF TEM and SAED images (Fig. 5a) confirms the presence of the β -phase with the $[001]$ zone axis (the same as the orientation of matrix). Moreover, BF TEM images present the martensitic plates and bright areas showing residual austenite. Fig. 5b shows a STEM HAADF micrograph and EDX and the elemental mapping of the NCAT sample after 10 superelastic

cycles. The EDX map indicates β plates enriched in Ni and Ta and depleted in Fe and Co, with a homogeneous distribution of Al. The chemical composition analysis is consistent with the literature data, where the composition of the β phase is $(\text{Ni})(\text{Al}, \text{Ta})$.

Fig. 6a shows BF TEM and SAED images for the NCATB sample after 10 superelastic cycles, indexed as γ austenite, with additional $\{100\}$ reflections corresponding to γ' phase. Similarly to the NCAT alloy, NCATB alloy also shows a dense dislocation microstructure, typical for materials subjected to cyclic deformation. However, the dislocation density is much smaller than for NCAT sample. The HRTEM image and the corresponding FFT as well as IFFT taken from the marked area are presented in Fig. 6b. The HRTEM image indicates the existence of fine γ' precipitates, as evidenced by a different contrast pointing to the lattice parameters change. Based on the FFT image, the γ phase with $\{200\}$ reflections is identified, while the weak peaks are related to the $\{100\}$ superstructure of the ordered γ' phase. The areas of γ' phase are marked with a green dashed line (IFFT), where the extra $\{100\}$ plane with a lattice spacing of 3.61 Å can be seen. Nevertheless, in the other places only the $\{200\}$ atomic planes with 1.80 Å lattice spacing were noticed. Additionally, the HRTEM image also shows a very good coherency between precipitations and the matrix. Furthermore, the average diameter of γ' precipitates, calculated based on DF and HRTEM observations, is found to be about 3 nm.

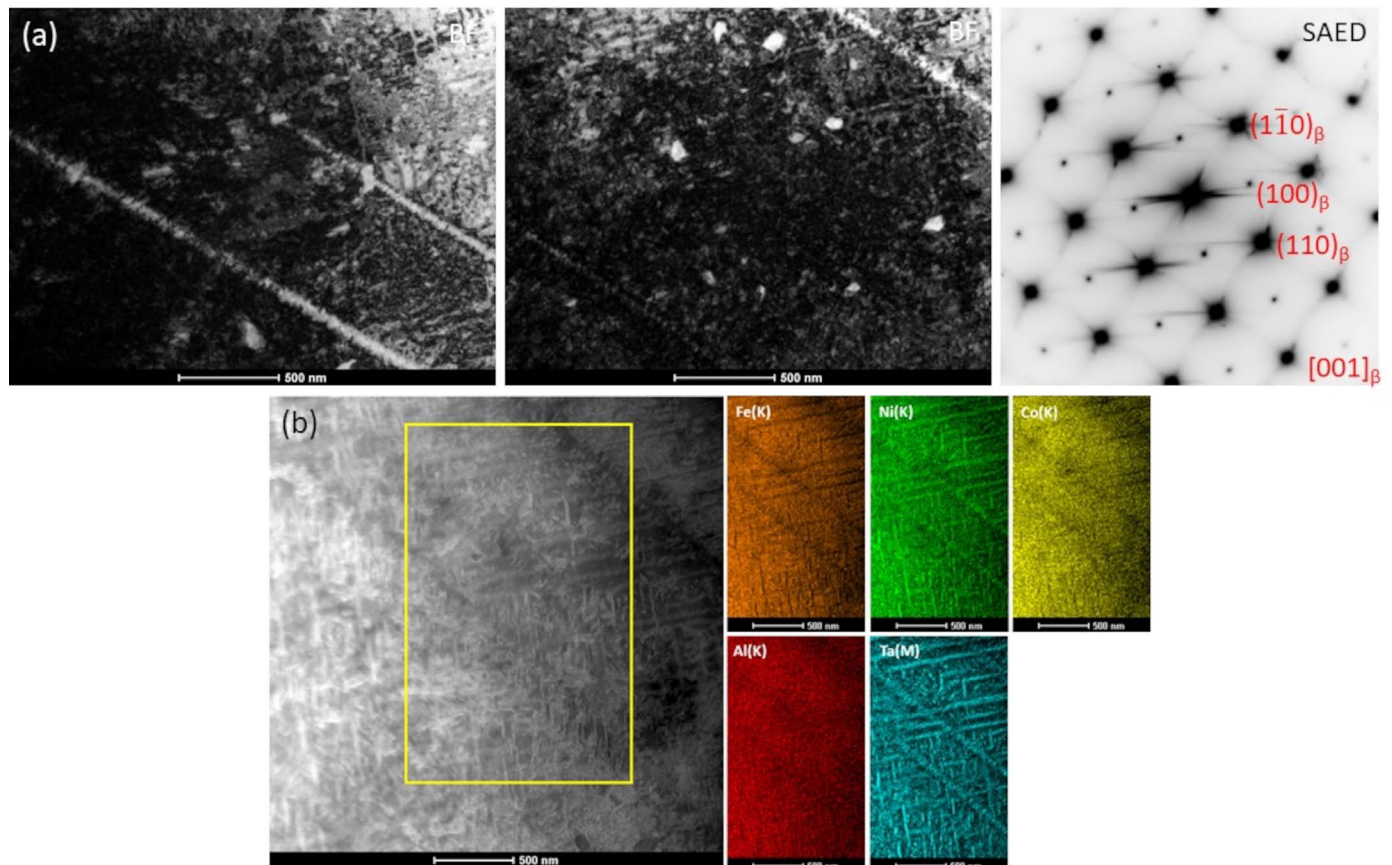


Fig. 5. (a) BF TEM images and corresponding SAED patterns and (b) STEM-HAADF image and EDX elemental mapping of NCAT sample after 10 superelastic cycles

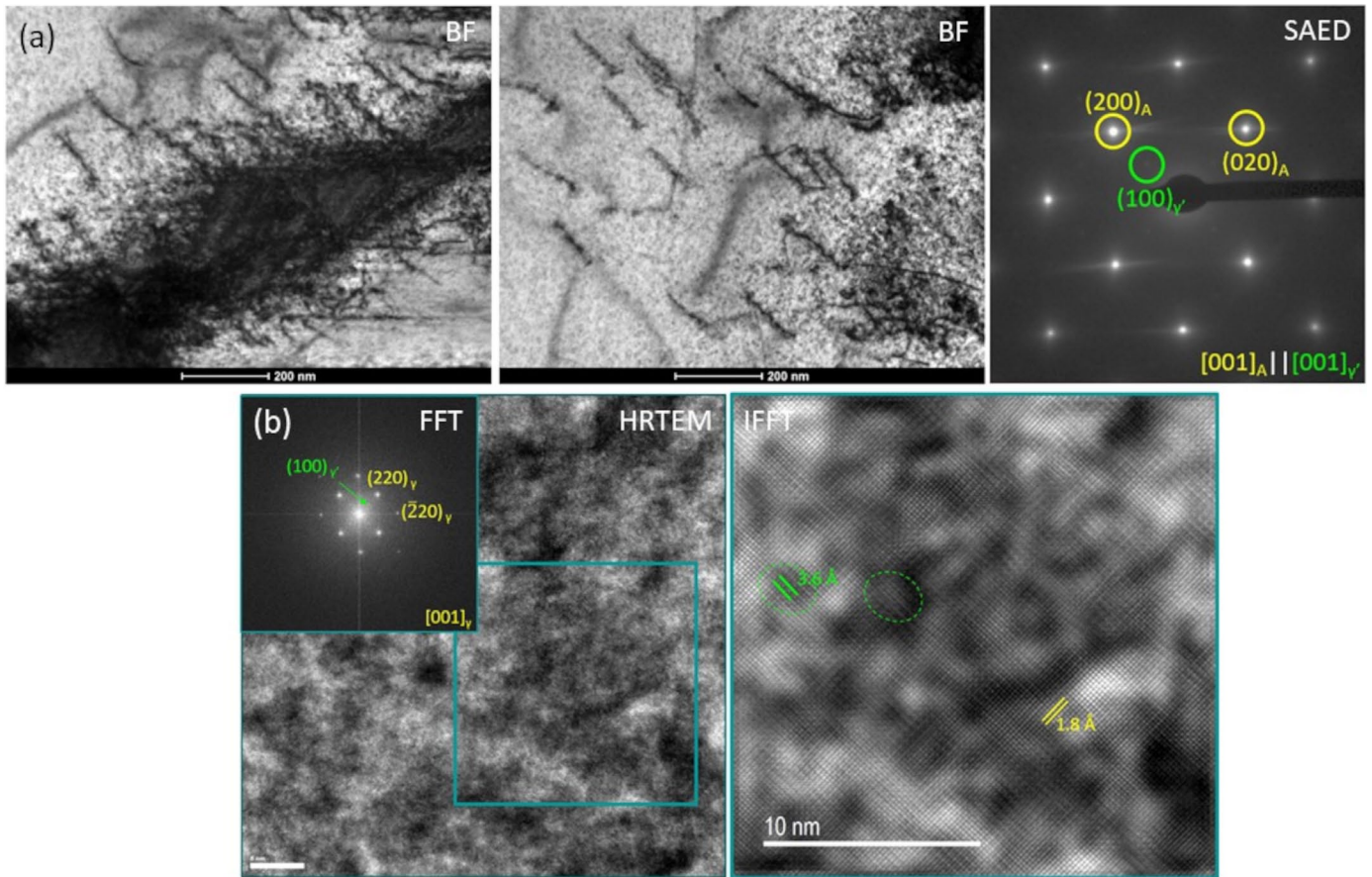


Fig. 6. (a) BF TEM images and corresponding SAED patterns and (b) HRTEM FFT and IFFT images of NCATB sample after 10 superelastic cycles

3.3. Discussion

The increase of dislocation density (visible in TEM micrographs) after each superelastic cycle leads to the gradual degradation of the material subjected to cyclic superelastic deformation. In the case of Ni-Ti alloys, the gradual degradation of the material is related to the stabilization of martensite caused by the anchoring of dislocations at the austenite-martensite interface. The increase of dislocation density, leading consequently to the irreversibility of the stress-induced martensitic transformation, results from the partly plastic (irreversible) nature of the deformation, which is caused by the high critical stress of the nucleation of the new phase [24–28]. However, the formation of residual martensite may be associated with a higher dislocation activity at the austenite/martensite interface, since small dislocation stress fields may pin the stress-induced martensite. On the other side, Simon et al. show that dislocations resulting from cyclic superelastic deformation have the mechanical energy required to retain/stabilize martensite [29]. Kroß et al. proposed two mechanisms accompanying the gradual cyclic degradation of Fe-based alloys. The first one concerns the increasing density of dislocations at the austenite/martensite interface, which cause mechanical anchoring of martensite plates – martensite stabilization. With the increasing number of dislocations, the volume fraction of the martensitic phase rises. The second mechanism is related to the pinning of martensite plates at the interfaces

of γ' precipitates/matrix [30]. Our results show that mechanical stabilization (complete compression which leads to single variant state of martensite) and related to that abrupt back transformation significantly increase the number of dislocations. This, in turn, degrades the functional properties of the material shifting A_s temperature with each cycle towards higher values. On the other hand, in NCATB single crystal which possesses smaller γ' precipitates (3 nm), the density of dislocation also increases, however, to a substantially lesser degree giving rise to more stable operation.

4. Conclusions

In this work, the influence of size and volume fraction of the γ' precipitates on the structural stability of two monocrystalline NCAT and NCATB alloys was investigated. The base NCAT alloy was characterized by a two-phase structure consisting of austenite and the γ' phase. The size of γ' precipitates was estimated at about 5 nm while the volume fraction was found to be 4 vol.%. The value of superelastic deformation was estimated at approx. 15%. In the case of the NCATB single crystal, the structure was also identified as two-phase: austenite + γ' phase. The size of the precipitates was 3 nm while the volume fraction was 2 vol.%. The size of the superelastic effect reached about 14%.

In both cases, with the increase in the number of superelastic cycles, the size of γ' precipitates remained unchanged while the volume fraction slightly increased. Moreover, the effect of training on the onset of martensitic transformation was clearly visible, with each successive superelastic cycle the martensitic transformation was induced by lower stress. As evidenced by microstructural observations, the dislocation density increased significantly. NCAT material returned to its original shape up to 9 superelastic cycles, whereas after 10 cycles it did not regain its original shape even after heating up to 773 K for 10 minutes. The annealing led to the formation of the β phase, which adversely affects the superelastic properties. In turn, the NCATB sample returned to its original shape at liquid nitrogen temperature even after 10 superelastic cycles. According to the obtained results and literature data, two mechanisms were found to be responsible for the cyclic degradation: the first one related to the increase of dislocations at the austenite/martensite interface, which causes the anchoring of martensite plates; the second is related to the pinning of the martensite plates at the austenite/ γ' precipitates interface.

Acknowledgement

The work was financed by the Institute of Metallurgy and Materials Science of the Polish Academy of Sciences within the statutory work Z-12/2021.

REFERENCES

- [1] Y. Tanaka, Y. Himuro, R. Kainuma, Y. Sutou, T. Omori, K. Ishida, Ferrous polycrystalline shape-memory alloy showing huge superelasticity, *Science* **327**, 1488 (2010). DOI: <https://doi.org/10.1126/science.1183169>
- [2] Y. Tanaka, Y. Himuro, T. Omori, Y. Sutou, R. Kainuma, K. Ishida, Martensitic transformation and shape memory effect in ausaged Fe-Ni-Si-Co alloys, *Mater. Sci. Eng. A* **1030**, 438-440 (2006). DOI: <https://doi.org/10.1016/j.msea.2006.02.103>
- [3] H. Sehitoglu, I. Karaman, X.Y. Zhang, Y. Chumlyakov, H.J. Maier, Deformation of FeNiCoTi shape memory single crystals, *Scr. Mater.* **44**, 779 (2001).
- [4] T. Maki, K. Otsuka, C.M. Wayman, *Shape memory materials*, 1998 Cambridge University Press, p. 117, Cambridge.
- [5] R. Hayashi, S.J. Murray, M. Marioni, S. Allen, R.C. O'Handley, Magnetic and mechanical properties of FeNiCoTi magnetic shape memory alloy, *Sens. Actuators* **81**, 219 (2000). DOI: [https://doi.org/10.1016/S0924-4247\(99\)00127-2](https://doi.org/10.1016/S0924-4247(99)00127-2)
- [6] T. Omori, K. Ando, M. Okano, X. Xu, Y. Tanaka, I. Ohnuma I.R. Kainuma, K. Ishida, Superelastic effect in polycrystalline ferrous alloys, *Science* **68**, 333 (2011). DOI: <https://doi.org/10.1126/science.1202232>
- [7] T. Maki, K. Kobayashi, M. Minato, I. Tamura, Thermoelastic martensite in an ausaged FeNiTiCo alloy, *Scr. Metall.* **18**, 1105 (1984). DOI: [https://doi.org/10.1016/0036-9748\(84\)90187-X](https://doi.org/10.1016/0036-9748(84)90187-X)
- [8] I.V. Kireeva, Y. Chumlyakov, V.A. Kirillov, I.V. Kretinina, Danil'son YuN, I. Karaman, *Russ. Phys. J* **53**, 10 (2011).
- [9] I.V. Kireeva, Y. Chumlyakov, V.A. Kirillov, I. Karaman, E. Cesari, *Tech. Phys. Lett.* **37**, 5 (2011).
- [10] Y. Tanaka, Y. Himuro, R. Kainuma, Y. Sutou, T. Omori, K. Ishida, Ferrous Polycrystalline Shape-Memory Alloy Showing Huge Superelasticity, *Science* **327**, 1488-1490 (2010). DOI: <https://doi.org/10.1126/science.1183169>
- [11] T. Omori, S. Abe, Y. Tanaka, D.Y. Lee, K. Ishida, R. Kainuma, *Scri. Mater.* **69**, (11-12) 812-815 (2013).
- [12] Y. Chumlyakov, I.V. Kireeva, E. Yu. Panchenko, E.G. Zakharova, V.A. Kirillov V.A, *Dokl. Phys.* **49**, 1 (2004).
- [13] J. Ma, B. Kockar, A. Evirgen, I. Karaman, Z.P. Luo, Y. Chumlyakov, *Acta Mater* **60**, 2186 (2012).
- [14] J. Ma, B.C. Hornbuckle, I. Karaman, G.B. Thompson, Z.P. Luo, Y. Chumlyakov, The effect of nanoprecipitates on the superelastic properties of FeNiCoAlTa shape memory alloy single crystals, *Acta Mater.* **61**, 3445 (2013). DOI: <https://doi.org/10.1016/j.actamat.2013.02.036>
- [15] Y. Geng, M. Jin, W. Ren, W. Zhang, X. Jin, Effects of aging treatment on martensitic transformation of Fe-Ni-Co-Al-Ta-B alloys, *J. Alloys Compd.* **577**, 631 (2012). DOI: <https://doi.org/10.1016/j.jallcom.2012.03.033>
- [16] P. Krooß, T. Niendorf, I. Karaman, Y. Chumlyakov, H.J. Maier, Cyclic Deformation Behavior of Aged FeNiCoAlTa Single Crystals, *Funct. Mater. Lett.* **5**, 4 (2012). DOI: <https://doi.org/10.1142/S1793604712500452>
- [17] P. Krooß, M. Holzweißig, T. Niendorf, C. Somsen, M. Schaper, Y. Chumlyakov, et al., Thermal cycling behavior of an aged FeNiCoAlTa single-crystal shape memory alloy, *Scr. Mater.* **81**, 28 (2014).
- [18] M. Czerny, W. Maziarz, G. Cios, A. Wojcik, Y. Chumlyakov, N. Schell, M. Fitta, R. Chulist, The effect of heat treatment on the precipitation hardening in FeNiCoAlTa single crystals, *Mater. Sci. Eng. A* **784**, 139327 (2020). DOI: <https://doi.org/10.1016/j.msea.2020.139327>
- [19] M. Czerny, G. Cios, W. Maziarz, Y. Chumlyakov, N. Schell, R. Chulist, Effect of B addition on the superelasticity in FeNiCoAlTa single crystals, *Mater. Design* **197**, 109225 (2021). DOI: <https://doi.org/10.1016/j.matdes.2020.109225>
- [20] M. Czerny, G. Cios, W. Maziarz, Y. Chumlyakov, R. Chulist, Studies on the Two-Step Aging Process of Fe-Based Shape Memory Single Crystals, *Materials* **13**, 1724 (2020). DOI: <https://doi.org/10.3390/ma13071724>
- [21] M. Czerny, Kraków 2021, The effect of crystallographic orientation of matrix and precipitation hardening on the superelastic strain in Fe-based shape memory alloys.
- [22] A. Wójcik, R. Chulist, P. Czaja, M. Kowalczyk, P. Zackiewicz P.N. Schell, W. Maziarz, Evolution of microstructure and crystallographic texture of Ni-Mn-Ga melt-spun ribbons exhibiting 1.15% magnetic field-induced strain, *Acta Mater.* **219**, 117237 (2021). DOI: <https://doi.org/10.1016/j.actamat.2021.117237>
- [23] R. Chulist, P. Czaja, On the role of atomic shuffling in the 4O, 4M and 8M martensite structures in Ni-Mn-Sn single crystal, *Scripta Mater.* **189**, 106 (2020). DOI: <https://doi.org/10.1016/j.scriptamat.2020.08.007>

- [24] K. Gall, H.J. Maier, Cyclic deformation mechanisms in precipitated NiTi shape memory alloys, *Acta Mater.* **50**, 4643 (2002). DOI: [https://doi.org/10.1016/S1359-6454\(02\)00315-4](https://doi.org/10.1016/S1359-6454(02)00315-4)
- [25] K. Gall, H. Sehitoglu, Y. Chumlyakov, I. Kireeva, Pseudoelastic cyclic stress-strain response of over-aged single crystal Ti-50.8at%Ni, *Scr. Mater.* **40**, 7 (1999).
- [26] K. Gall, H. Sehitoglu, R. Anderson, I. Karaman, Y. Chumlyakov, I. Kireeva, On the mechanical behavior of single crystal NiTi shape memory alloys and related polycrystalline phenomenon, *Mater. Sci. Eng. A* **317**, 85 (2001).
- [27] R. Delville, B. Malard, J. Pilch, P. Sittner, D. Schryvers, Transmission electron microscopy investigation of dislocation slip during superelastic cycling of Ni-Ti wires, *Int. J. Plast.* **27**, 282 (2011). DOI: <https://doi.org/10.1016/j.ijplas.2010.05.005>
- [28] J. Zhang, C. Somsen, T. Simon, X. Ding, S. Hou, S. Ren, X. Ren, G. Eggeler, K. Otsuka, J. Liu, Leaf-like dislocation substructures and the decrease of martensitic start temperatures: A new explanation for functional fatigue during thermally induced martensitic transformations in coarse-grained Ni-rich Ti-Ni shape memory alloys, *Acta Mater.* **60**, 1999 (2012). DOI: <https://doi.org/10.1016/j.actamat.2011.12.014>
- [29] T. Simon, A. Kroeger, C. Somsen, A. Dlouhy, G. Eggeler, On the multiplication of dislocations during martensitic transformations in NiTi shape memory alloys, *Acta Mater.* **58**, 1850 (2010). DOI: <https://doi.org/10.1016/j.actamat.2009.11.028>
- [30] P. Krooß, C. Somsen, T. Niendorf, M. Scharper, I. Karaman, Y. Chumlyakov, G. Eggeler, H.J. Maier, Cyclic degradation mechanisms in aged FeNiCoAlTa shape memory single crystals, *Acta Mater.* **79**, 126-137 (2014). DOI: <https://doi.org/10.1016/j.actamat.2014.06.019>